Graph-based Pigment Network Detection in Skin Images

M. Sadeghi [a,b] , M. Razmara [a], M. Ester [a], T. K. Lee [a,b,c], M. S. Atkins [a]

[a]Simon Fraser University, 8888 University Drive, Burnaby, BC, Canada, V5A1S6;
[b]Cancer Control Research, BC Cancer Agency, 675 W. 10th Ave., Vancouver, Canada V5Z1L3
[c]Photomedicine Institute, Department of Dermatology and Skin Science, University of British Columbia, and Vancouver Coastal Health Research Institute, Canada

ABSTRACT

Detecting pigmented network is a crucial step for melanoma diagnosis. In this paper, we present a novel graph-based pigment network detection method that can find and visualize round structures belonging to the pigment network. After finding sharp changes of the luminance image by an edge detection function, the resulting binary image is converted to a graph, and then all cyclic sub-graphs are detected. Theses cycles represent meshes that belong to the pigment network. Then, we create a new graph of the cyclic structures based on their distance. According to the density ratio of the new graph of the pigment network, the image is classified as "Absent" or "Present". Being *Present* means that a pigment network is detected in the skin lesion. Using this approach, we achieved an accuracy of 92.6% on five hundred unseen images.

Keywords: Dermoscopy, skin lesion, pigment network detection,texture analysis, graph, cyclic sub-graph.

1. INTRODUCTION

The incidence of malignant melanoma, a disease of worldwide distribution, has been rapidly increasing over the last few decades, especially among Caucasians.[1–4] Early detection and prompt surgery represent the only curative management of patients affected by the disease. When melanoma is found in an early stage, the chances for long-term survival are excellent. Five-year survival rates for patients with early-stage (Stage I) melanoma exceed 90 to 95%. As melanoma progresses, it becomes increasingly more deadly. In later-stage disease, 5-year survival rates drop to less than 50%.[5] Therefore, there is a need to develop computer-aided diagnostic systems to facilitate the early detection of melanoma. The first step in these systems is skin lesion segmentation which is widely addressed in the literature.[6, 7]

The clinical diagnosis of melanoma is commonly based on the ABCD system, which is a checklist of important parameters.[8] This technique focuses on asymmetry, irregular border, number of colors (associated also to slate blue veil and whitish veil), and the presence of differential structures (streaks, globular elements, etc.). The guideline requires computing a weighted score of these features. However, the method in practice usually helps in focusing on the most important parameters during a skin lesion examination. The parameter evolution is usually considered, becoming the "ABCDE rule". There is another method proposed by Menzies and co-workers in 1996.[9] This method is based on a couple of features which are important for making diagnosis such as the presence of irregular border, irregular pigmented network, abrupt cut-off of the network, streaks, globular elements and colors. Colour features used for lesion scoring include blue-white veil, red-blue areas, multiple coloration, brown dots and globules, blue /gray dots, and many more.[9]

Therefore, according to the mentioned methods, melanomas usually have features indicating their melanocytic origin such as:

- Pigment network

- Aggregated brown, or black globules

- Site-specific features e.g. parallel pattern on palms and soles, follicular openings on facial skin

Many other features have been found in melanoma, and they may be relatively featureless. Superficial melanomas often have one or more of the following dermoscopic features:

- Broad pigment network

- Blue-white veil

- Multiple brown dots

- Pseudopods

- Radial streaming

- Multiple (5-6) colours, especially red and blue

- Peripheral black dots/globules

- Negative network

- Irregular vascularity

- Scar-like depigmentation

- Focal sharply cut-off border

Recently, a new technology has been introduced, known as dermoscopy or epiluminescence microscopy (ELM).[10] It is a non-invasive in vivo technique that permits visualization of features of pigmented melanocytic neoplasms that are not perceivable by examination with the naked eye. Using this new technique a completely new range of visual features such as the pigment network, solid pigment, radial streaming, globules, blue/gray veil, etc. can be visualized to aid the diagnostic process.

There are some texture and color features which describe the malignancy or other types of the skin cancer. Atypical pigment network is one of the crucial features of a malignant lesion. The pigment network seen in melanocytic lesions stems from increased melanin content in keratinocytes or melanocytes outlining the rete ridges pattern of the epidermis. The holes in the network correspond with the epidermal suprapapillary plates.[11, 12] Our addressed problem is how to determine the absence or presence of pigment networks in a given skin lesion image.

A typical pigment network is defined as "a light-to-dark-brown network with small, uniformly spaced network holes and thin network lines distributed more or less regularly throughout the lesion and usually thinning out at the periphery".[13]

Our proposed method is a robust, reliable, computer-aided diagnostic tool for analyzing the texture in lesions of the skin to detect pigment networks in the presence of other structures such as dots and globules. The goal is to classify a given image to two classes: *Present* or *Absent*, that has qualitative information about the absence or presence of the pigment network. Figure 1 shows two examples of *Absent* and *Present* lesions.

Detection of the pigment network has been investigated recently.[10, 14–17] Anantha et al. propose two algorithms for detecting pigment networks in skin lesions: one involving statistics over neighboring gray-level dependence matrices, and one involving filtering with Laws energy masks.[14] Various Laws masks are applied and the responses are squared. Improved results are obtained by a weighted average of two Laws masks whose weights are determined empirically. Classification of these tiles is done with approximately 80% accuracy. Betta et al. begin by taking the difference of an image and its response to a median filter.[15] This difference image is thresholded to create a binary mask which undergoes a morphological closing operation to remove any local discontinuities. This mask is then combined with a mask created from a high-pass filter applied in the Fourier domain to exclude any slowly modulating frequencies. Results are reported graphically, but appear to achieve a sensitivity of 50% with a specificity of 100%.

In 2006, Betta et al.[16] proposed an approach to detect and localize network patterns. Such texture is automatically detected with Gaussian derivative kernels and Fisher linear discriminant analysis; line closure and thinning is provided by morphological masking and line luminance profile fitting provides width estimation. An overall 88.3% network detection performance is reported on dermatological images. Even though high contrast
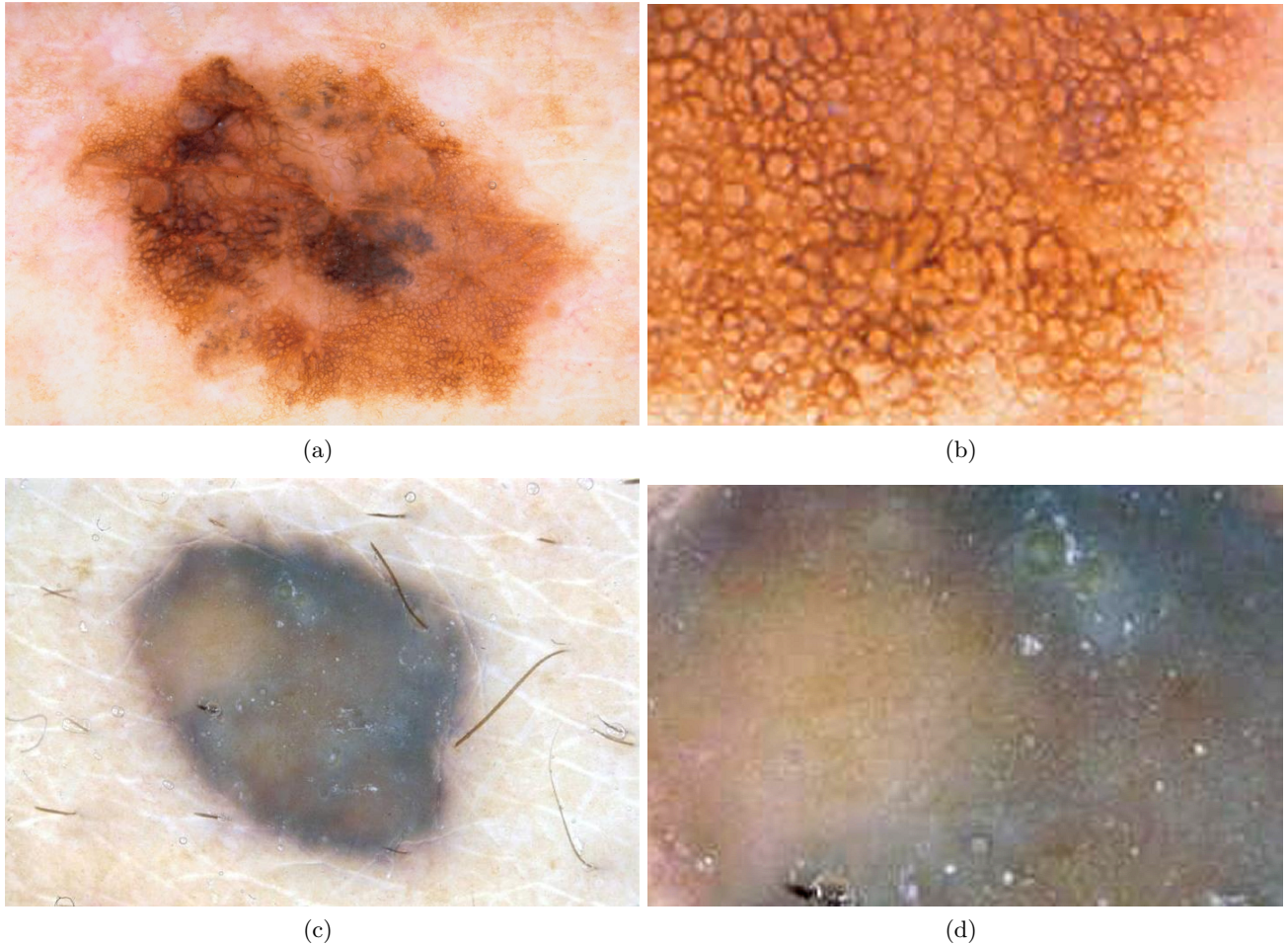
Figure 1. a) Present: A lesion containing a pigment network. b) An enlarged pigment network . c) Absent: An image of a lesion without pigment network

images are used to visualize results of the method, there are false positives which are hair lines or noise. They could consider spatial arrangements of network holes to remove false positives.

In a recent work, Serrano et. al.[17] present a new methodology to classify the lesions, not focused on the extraction of specific shape, texture or colour features, but performing a pattern recognition step. The lesion is classified into five different types of patterns which are reticular pattern or network pattern, globular pattern, cobblestone pattern, homogeneous pattern, and parallel pattern. For doing the analysis of the colour textured pattern, they model the image as a finite symmetric conditional Markov (FSCM) model, and calculate a feature vector with the parameters of the model. They employ different colour spaces and show that the L*a*b* colour space outperforms the others. To obtain the label assigning the type of the pattern, the maximum likelihood (ML) criterion is applied to maximize the conditional probability distribution. The inputs to the algorithm are 40x40 pixel images corresponding to a particular type of pattern, and the output is the class of the pattern. It is a supervised method due to the availability of a training set. The correct classification rate achieved is of 90% for the reticular pattern (pigment network) and 86% on average.

2. PROPOSED APPROACH

We analyze a set of lesion images each with a label (*Absent* or *Present*) representing the presence of a pigment network in the image. The specific location of the pigment network structure within the image is found and visualized. Then, the image is classified according to the ratio of the pigment network presence.

This paper explores a novel graph-based approach which includes following steps: First, in order to prevent unnecessary analysis of the pixels belonging to the skin, the lesion is manually segmented by an expert. Next, the quality of the image is enhanced to highlight the texture features. For sharpening, we created two-dimensional high-pass filter coefficients suitable for correlation. A 3-by-3 contrast enhancement filter created from the negative of the Laplacian filter with parameter α is used. α controls the shape of the Laplacian and must be in the range 0.0 to 1.0. Our default value for alpha is 0.2. Then, the image is converted to a luminance image using

$$Y = 0.299R + 0.587G + 0.114B$$

where Y is the luminance and R, G and B are the red, green, and blue color components, respectively. Afterwards, sharp change of intensity is detected using the Laplacian of Gaussian (LOG) filter. Result of this edge detection step is a binary image which is subsequently converted into a graph to find meshes or cyclic structures of the lesion. After finding loops or cyclic subgraphs of the graph, noise or undesired cycles are removed and a graph of the pigment network is created using the extracted cyclic structures. According to the density of the pigment network graph, the given image is classified into *Absent* or *Present*. Figure 2 shows the overall structure of this system.

2.1 Feature Extraction

The presence of atypical pigment network is indicated by "black, brown, or gray network with irregular meshes and thick lines" and a typical pigment network is defined as a "light- to dark-brown network with small, uniformly spaced network holes and thin network lines distributed more or less regularly throughout the lesion and usually thinning out at the periphery". These structures show prominent lines, homogeneous or inhomogeneous meshes. From an image processing point of view, these structures can be detected firstly by searching for the occurrence of the texture and consequently by evaluating its possible chromatic and spatial evolution. To extract these key features we search for round or cyclic structures which represent the presence of the pigment network. To find the meshes or cyclic structures in the luminance image, it is necessary to detect sharp changes of the intensity. Because of the inherent properties of Laplacian of Gaussian (LOG) filter, it can detect the "light-dark-light" changes of the intensity well. The detection criterion is the presence of a zero crossing in the second derivative with the corresponding large peak in the first derivative.

$$h(x,y) = \triangle^2[g(x,y) * f(x,y)] = [\triangle^2 g(x,y)] * f(x,y)$$

$$\triangle^2 g(x,y) = \left(\frac{x^2 + y^2 - 2\sigma^2}{\sigma^4} \right)^{\frac{-(x^2+y^2)}{2\sigma^2}}$$

Setting the threshold to zero, we obtain an edge image with closed contours of zero-crossings in the input image. The next step is to detect the meshes or round structures in the edge image. In the previous works[15, 16] these structures usually are found by morphologic techniques and a sequence of closing and opening functions were applied to the black and white image. We did not use this approach because using morphologic technique is error-prone in detecting the round shape structures. So, having a binary image of the connected components (the edges of the images), we convert them to a Graph (G_i) with 8-connected neighbors. Each pixel in the connected component is a node of G_i and each node has a unique label according to its coordinate.

To find the cyclic texture features, all cyclic subgraphs are detected using the Iterative Loop Counting Algorithm (ILCA).[18] This algorithm transforms the network into a tree and does a depth first search on the tree for loops. After finding cyclic subgraphs which represent meshes of the skin texture that could possibly belong to a pigment network, they were filtered and noise or wrongly detected structures (globules and dots) were removed according to the prior knowledge about the shape, size and color of the meshes of pigment network. In globules, color of the inside area of the structure is darker than the border pixels or the outside area. Therefore, by setting
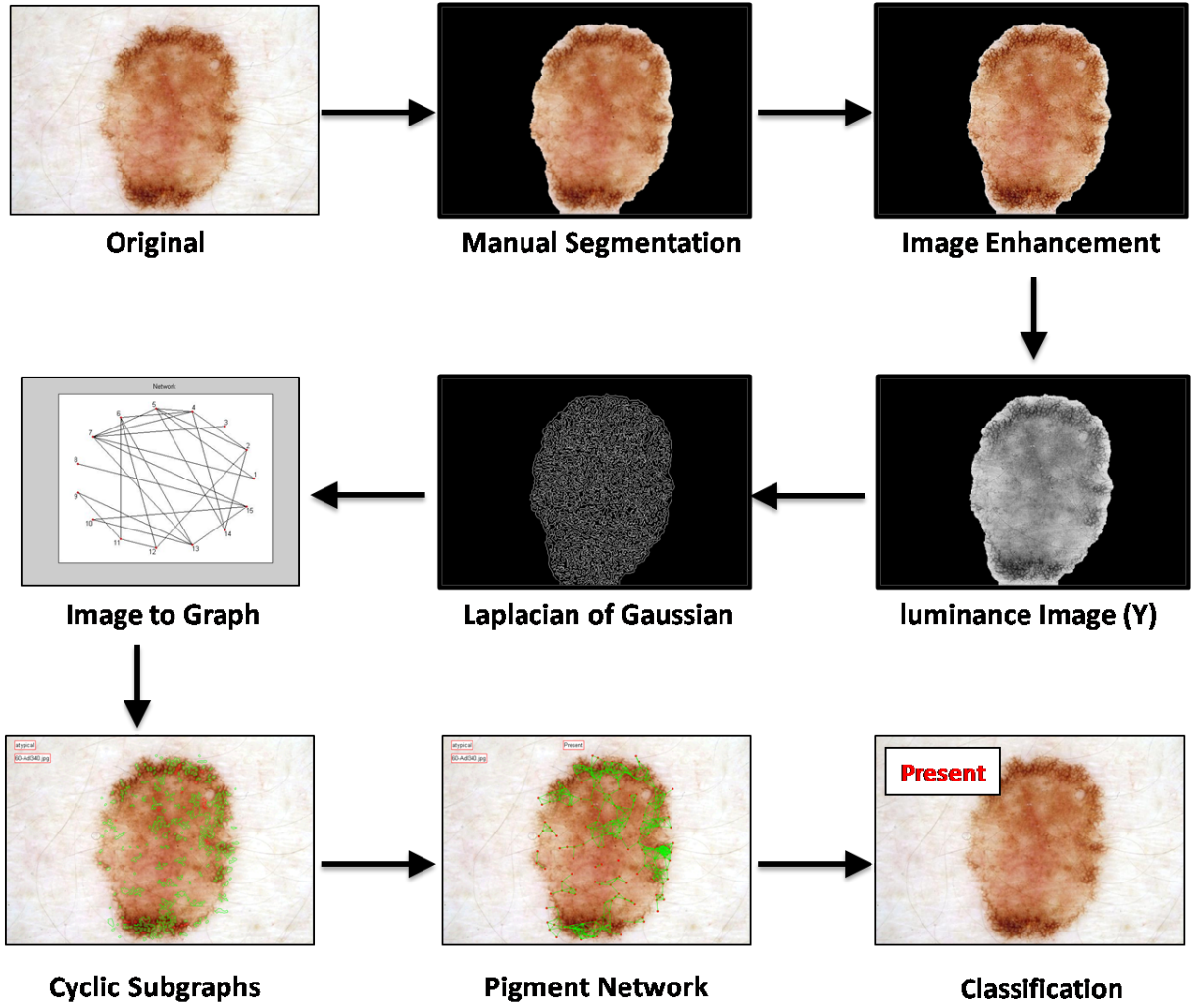
Figure 2. Overview of the proposed algorithm which has the following steps for a given image of a skin lesion. Original image ⟶manual segmentation of the lesion ⟶ image enhancement (sharpening) ⟶ illuminance image (RGB to Y) ⟶ Laplacian of Gaussian ⟶ image to graph conversion ⟶ finding cyclic subgraphs ⟶ create pigment network graph ⟶ classification.

a threshold for the difference between the average color of border pixels and the average color of the inside area, we can discriminate globules from meshes of the pigment network.

In order to visualize the graph of a pigment network, we created a new graph whose nodes are centers of the meshes belonging to the pigment network. Considering spatial arrangement of holes of the pigment network, we set a threshold for their Euclidean distance. Nodes within a maximum distance threshold (MDT) are connected together.

To classify images into *Absent* and *Present*, we defined a density ratio as

$$Density = \frac{|E|}{(|V| * \log(LesionSize))}$$

where E is the number of edges in the graph, V is the number of nodes of the graph and *LesionSize* is the size of the area of the image investigated for finding the pigment network. Images containing a density ratio higher than a threshold (set to 1.5) are classified as *Present* and the rest as *Absent*.

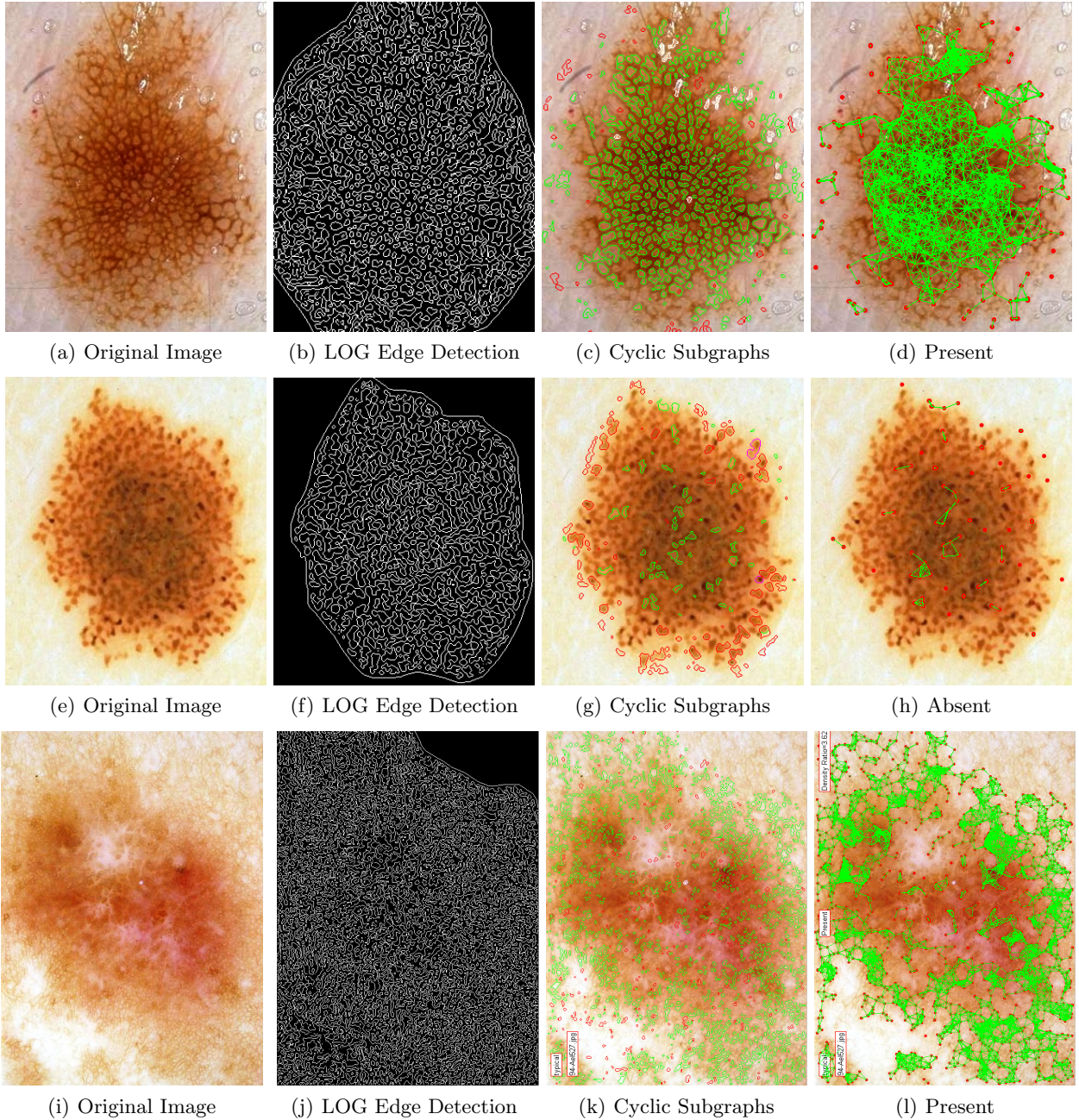|			
(a) Original Image	(b) LOG Edge Detection	(c) Cyclic Subgraphs	(d) Present
(e) Original Image	(f) LOG Edge Detection	(g) Cyclic Subgraphs	(h) Absent
(i) Original Image	(j) LOG Edge Detection	(k) Cyclic Subgraphs	(l) Present

Figure 3. The first row shows a Present image, the second row shows an Absent image, and the third row shows another Present image, all of which are classified correctly. In Figure 3, (a), (e) and (i) are skin lesions, (b), (f) and (j) show the binary edge-detected images, (c), (g) and (k) show the cyclic subgraphs where the green meshes represent potential holes of the pigment network and red meshes could not pass the test of belonging to the pigment network, and (d), (h) and (l) visualize the pigment network over the image.

3. EVALUATION AND RESULTS

We applied our method to a set of dermoscopic images taken from Argenziano et al.'s Interactive Atlas of Dermoscopy.[19] We tuned the parameters and thresholds of our proposed method according to a set of 100 images of size 768x512. Then we tested the method for another set of images (500 images) randomly selected from the atlas. All images of the training and the test set were labeled as *Absent* or *Present* by experts in the

atlas. Some of these images were challenging due to acquisition parameters such as lighting and magnification, being partial (entire lesion was not visible), or the presence of an unreasonable amount of occlusion by either oil or hair. These challenging images are usually discarded from test sets in the previous works. However, these images were kept in our test set.

The accuracy of our pigment network detector is 92.6% for 500 images in the test set. Figure 3 shows some of our experimental results. The first row shows a Present image, the second row shows an Absent image, and the third row shows another Present image, all of which are classified correctly. In Figure 3, (a), (e) and (i) are skin lesions, (b), (f) and (j) show the binary edge-detected images, (c), (g) and (k) show the cyclic subgraphs where the green and red meshes represent the potential holes of the pigment network and rejected round objects respectively, and (d), (h) and (l) visualize the pigment network over the image. Our system outperforms Anantha et al. 's method[14] where their accuracy is 80% for the 2-class classification.

4. CONCLUSION AND FUTURE WORK

We proposed a novel graph-based method for classifying and visualizing pigment networks and validated the method by evaluating its ability to classify and visualize the real dermoscopic images. The accuracy of the system is 92.6% in classifying images to two classes of *Absent* and *Present*. This method can be used as a part of an automatic diagnosis system for classifying moles and skin cancer detection. In addition, extracted features can be used in skin lesion segmentation systems. This is a novel idea that needs more investigation and evaluation and has a good potential for the future research. This method will be extended to classify images into 3-classes: Absent, Typical, and Atypical. We also believe the approach can be used to extract other skin patterns.

5. ACKNOWLEDGEMENTS

REFERENCES

[1] *Canadian Cancer Society's Steering Committee, Canadian Cancer Statistics, 2009, Toronto, Canada* (2009).

[2] Jemal A, Murray T, W. E., "Cancer statistics, 2005," *CA Cancer J Clin* **55**, 10–30 (September 2005).

[3] *Cancer facts and figures 2009, American Cancer Society, Atlanta* (2009).

[4] M., L. and Dawes, M., "Global perspectives of contemporary epidemiological trends of cutaneous malignant melanoma," *British Journal of Dermatology* **150**, 179–185 (2004).

[5] Balch CM, B. A., "Final version of the american joint committee on cancer staging system for cutaneous melanoma," *Journal of clinical oncology : official journal of the American Society of Clinical Oncology.* **19**, 3635–3648 (August 2001).

[6] Celebi, E., M., Aslandogan, A., Stoecker, William, V., Iyatomi, Oka, H., Hiroshi, Chen, and Xiaohe, "Unsupervised border detection in dermoscopy images," *Skin Research and Technology* **13**, 454–462 (November 2007).

[7] Wighton, P., Sadeghi, M., Lee, T. K., and Atkins, M. S., "A fully automatic random walker segmentation for skin lesions in a supervised setting.," in [*MICCAI (1)*], *Lecture Notes in Computer Science* **5762**, 1108–1115, Springer (2009).

[8] Friedman R J, R. D. S. and W, K. A., "Early detection of malignant melanoma: the role of the physician examination and self examination of the skin," *CA Cancer J Clin* **35**, 130151 (May 1985).

[9] Menzies, S. W., "A method for the diagnosis of primary cutaneous melanoma using surface microscopy," *Dermatologic Clinics* **19**, 299–305 (2001).

[10] Braun, R. P., French, L. E., and Saurat, J.-H., "Dermoscopy of pigmented lesions: a valuable tool in the diagnosis of melanoma," *SWISS MED WKLY* **134**, 83–99 (2004).

[11] Yadav S, Vossaert KA, K. A., "Histopathologic correlates of structures seen on dermoscopy (epiluminescence microscopy)," *Am J Dermatopathol* **15**, 297–305 (1993).

[12] Massi D, De Giorgi V, S. H., "Histopathologic correlates of dermoscopic criteria," *Dermatologic Clinics* **19**, 259–268 (2001).

[13] H. P. Soyer, G. A. e. a., "Dermoscopy of pigmented skin lesions: Results of a consensus meeting via the internet," **48**(5), 679–693 (2003).

[14] Anantha, M., Moss, R. H., and Stoecker, W. V., "Detection of pigment network in dermatoscopy images using texture analysis," *Computerized Medical Imaging and Graphics* **28**, 225–234 (July 2004).

[15] Betta, G., Di Leo, G., Fabbrocini, G., Paolillo, A., and Sommella, P., "Dermoscopic image-analysis system: estimation of atypical pigment network and atypical vascular pattern," in [*MEMEA '06: Proceedings of the IEEE International Workshop on Medical Measurement and Applications*], 63–67 (2006).

[16] Grana, C., Cucchiara, R., Pellacani, G., and Seidenari, S., "Line detection and texture characterization of network patterns," in [*ICPR '06: Proceedings of the 18th International Conference on Pattern Recognition*], 275–278, IEEE Computer Society, Washington, DC, USA (2006).

[17] Serrano, C. and Acha, Bego n., "Pattern analysis of dermoscopic images based on markov random fields," *Pattern Recogn.* **42**(6), 1052–1057 (2009).

[18] Kirk, J., "Count loops in a network." `http://www.mathworks.com/matlabcentral/fx_files/10722/1/content/html/run_loops_html.html`, 'accessed on May 12, 2009'.

[19] Argenziano, G. and H. Soyer, e. a., [*Interactive Atlas of Dermoscopy (Book and CD-ROM)*], Edra medical publishing and new media (2000).